MNRAS **000**, 1–10 (2011) Preprint 7 August 2022 Compiled using MNRAS LATEX style file v3.0

Rotation of hot normal, peculiar and Be stars from space photometry

L. A. Balona
South African Astronomical Observatory, P.O. Box 9, Observatory, Cape Town, South Africa

Accepted .... Received ...

ABSTRACT
The periods of 34,376 main sequence stars hotter than 6000 K are derived from *Kepler, K2* and *TESS* light curves. From the effective temperatures and *GAIA DR3* luminosities, the radii and hence the equatorial rotational velocities, v, can be estimated. Comparison with the projected rotational velocities, $v \sin i$, shows that the photometric periods are the rotational periods. The distributions of v in different temperature ranges are shown to closely resemble the distributions of $v \sin i$. Rotational light modulation occurs in about 20–50 percent of stars in the upper main sequence. The rotation rates of Am, Ap and Bp stars do not appear to be very different from those of non-peculiar stars. Mixing of the surface layers by rotation cannot therefore be the sole reason why element diffusion does not occur in stars with normal surface abundances. From the distribution of rotational velocities of Be stars, it is shown that they typically rotate well below the rate required to trigger mass loss by nonradial pulsation. Surface activity leading to ejection of material into co-rotating clouds is suggested as the mass-loss mechanism. The trapped clouds lead to incoherent short-period, large amplitude variations, as observed. The rotational amplitudes of non-Be stars increases rapidly with effective temperature, possibly due to an increasing proportion of incipient Be stars in the sample. These results imply a need for revision of current ideas regarding atmospheres of hot stars.

Key words: stars:early type; stars: rotation; stars:starspots; stars:chemically peculiar; stars: emission-line, Be

1 INTRODUCTION

Observations from the *Kepler* and *TESS* space missions indicate that a considerable fraction of main sequence A and B stars vary in light with periods typical of their rotation periods (Balona 2011, 2013; Balona et al. 2015; Balona 2016, 2017; Balona et al. 2019; Sikora et al. 2020; Balona 2021). Their periodograms show a single isolated peak, sometimes accompanied by one or two harmonics, with amplitudes mostly smaller than one millimagnitude. Even a brief look at the light curves and periodograms from *Kepler* or *TESS* is enough to show that this is a common phenomenon which occurs all over the main sequence from cool stars to the hottest main sequence B stars.

It is generally accepted that starspots are responsible for rotational light modulation in cool stars (Hall 1972; Strassmeier 2009). However, it has long been supposed that stars with effective temperatures hotter than about 7500 K cannot host spots similar to those in the Sun. In these stars, surface convection is thought to be absent. The dynamo mechanism, which is responsible for generating surface magnetic fields in cool stars (Charbonneau 2014), is therefore unable to operate.

The *Kepler* mission was confined to a field with very few late B stars and almost no early B stars. To enable the rotational modulation hypothesis to be tested for B stars requires observations at low galactic latitudes. For this reason, *TESS* observations are very important. Previous work using just a few *TESS* sectors (Balona et al. 2019; Balona 2019) showed that rotational modulation is likely to be present, not only among A stars, but also in B stars. In a later study of Be stars, Balona & Ozuyar (2021) used *TESS* data for sectors 1–26 which began to show significant results for early B stars. In this paper we use all available *Kepler*, *K2* and *TESS* data for sectors 1–52 to test the rotational modulation hypothesis for B stars.

In stars with quiescent radiative envelopes, heavier elements experience a downwards drift, whereas radiation pressure acts to create an upwards drift of some atomic species relative to others. In the absence of convection, meridional circulation and other mixing, a vertical stratification of the elements will result. This diffusion process is the generally accepted explanation for the metallic-lined

Am stars (Michaud et al. 1976, 1983) in which a global magnetic field is weak or absent. The same process, operating in the presence of a strong global magnetic field, is thought to be responsible for the patches of anomalous abundances in chemically peculiar Ap and Bp stars (Michaud et al. 1976; Michaud 1980). The kilogauss global magnetic fields in Ap and Bp stars are presumed to be of fossil origin (Braithwaite & Spruit 2004).

The diffusion model for Ap and Bp stars requires low rotational velocities, otherwise mixing caused by meridional circulation would tend to eliminate the chemical peculiarities. In the past, the distribution of rotational velocities has been derived from the projected rotational velocities, $v \sin i$. This requires spectroscopic observations of fairly high dispersion, thus limiting the number of stars that can be used. There are now a large number of both peculiar and normal A and B stars in which the rotation periods can be directly derived from light modulation. In this paper, these observations are used to investigate how rotation in various types of chemically peculiar stars differs from normal main sequence stars. In this way, the prediction of the diffusion model can be tested.

Finally, *TESS* observations show that about 75 percent of Be stars have very distinctive light curves and periodograms and are easily identified. The pattern in the periodogram can also be used to identify what is probably the rotation period (Balona & Ozuyar 2020, 2021). The periodogram features are always broad because the photometric period varies slightly with time and does not maintain the same phase. In a minority of stars sharp peaks due to SPB or β Cep pulsations are present in addition to the broad peaks. In this paper we use all available *TESS* data to determine the distribution of v/v_c, the ratio of equatorial rotational velocity to the critical rotational velocity. This allows a test of the idea that the mass loss in Be stars is triggered by pulsation. For this mechanism to work, all Be stars must be rotating in excess of 95 percent of critical velocity (Townsend et al. 2004).

2 DATA AND ANALYSIS

Light curves from the full four-year *Kepler* mission and from sectors 1–52 of the *TESS* mission were used. These data are corrected using pre-search data conditioning (PDC). For the *K2* data, light curves corrected by the method described in Vanderburg & Johnson (2014) were used. The periodogram of each star was calculated and frequencies extracted. The light curves and periodograms were visually inspected and, where appropriate, a variability type was assigned using the classification scheme in the *General Catalogue of Variable Stars, GCVS* (Samus et al. 2018). Variability classification for nearly 118,000 stars observed by these three space missions were made.

Suspected rotational variables are identified by the presence of a solitary low-frequency peak in the periodogram with a frequency lower than about $5\,\mathrm{d}^{-1}$ or by a peak and one or more harmonics. Of course, such a peak is not easily distinguished from a low-level grazing eclipse or by an eclipse by a sub-stellar companion or planet.

In the *Kepler* data, where the time span is about four years, one can often deduce that the periodogram peak is relatively broad, indicative of quasi-periodic variations which can also be distinguished in the light curve. Indeed, the spread in frequency was used to study differential rotation in *Kepler* stars (Balona & Abedigamba 2016).

The limited time span of the *K2* and *TESS* data do not allow this method of discrimination between eclipses and rotation. For this reason rotation was assigned only if the peak amplitude is less than about 10 mmag. This does not eliminate the possibility of eclipses, of course, and the data are almost certainly contaminated by stars with low-level eclipses. Since the GCVS does not include a class for early-type rotational variables, the preliminary designation ROT was employed. The restriction on the maximum peak amplitude does not apply to the chemically peculiar α CVn (ACV), or SX Ari (SXARI) stars, because the light variation is due to chemical spots. It is also not applied to Be stars because the periodic variation is suggested to be a result of co-rotating clouds rather than starspots.

The test for significance of a frequency peak is based on its signal-to-noise ratio. The criterion of S/N $>$ 4 (Breger et al. 1993) has been widely used in the past, but is probably too optimistic (Baran et al. 2015; Baran & Koen 2021; Bowman & Michielsen 2021). Here we use the criterion S/N$>$ 4.7.

The sample of stars selected for analysis was chosen mainly on the availability of spectral classification. Nearly all recent photometry excludes the U band, which means that one cannot differentiate between A and B stars on photometry alone. Indeed, the effective temperatures in the *Kepler Input Catalogue* (Brown et al. 2011) or the *TESS Input Catalog* (Stassun et al. 2018) are unreliable for B stars.

A catalogue was created which includes the variability class, the effective temperature, luminosity, rotation period, spectral type and other useful parameters. It also includes the projected rotational velocity, $v \sin i$, mainly from Głębocki & Gnaciński (2005), but supplemented by more recent values from the literature. Effective temperatures, $T_{\rm eff}$ were derived from the literature and allocated priorities. For example, values of $T_{\rm eff}$ from spectral line fitting were allocated the highest priority. Those derived from narrow-band photometry are given lower priority, etc. When no other option was available, an estimate of $T_{\rm eff}$ from the spectral type and luminosity class was made. The adopted $T_{\rm eff}$ is the average of those values which were allocated the highest priority.

Luminosities for all stars were derived from *Gaia* DR3 parallaxes (Gaia Collaboration et al. 2016, 2022) using the *Gaia* G magnitude and corresponding bolometric correction from Chen et al. (2019). The interstellar extinction in G is taken from (Anders et al. 2022) which is based on a 3D extinction map by Green et al. (2019). For the few stars that are not listed in the catalogue by Anders et al. (2022), the 3D extinction map by Gontcharov (2017) was used. The typical error in $\log L/L_\odot$ is 0.07 dex which includes the error in the parallax, an error of 0.02 mag in G, and an error of 0.05 mag in both the extinction, A_G, and the bolometric correction.

The equatorial rotational velocity, v, is estimated from the photometric rotation period and the stellar radius derived from $T_{\rm eff}$ and $\log L/L_\odot$. The error in v is determined mainly by the error in $T_{\rm eff}$ and is estimated to be about $40\,\mathrm{km\,s}^{-1}$. The typical error in $v \sin i$ is approximately

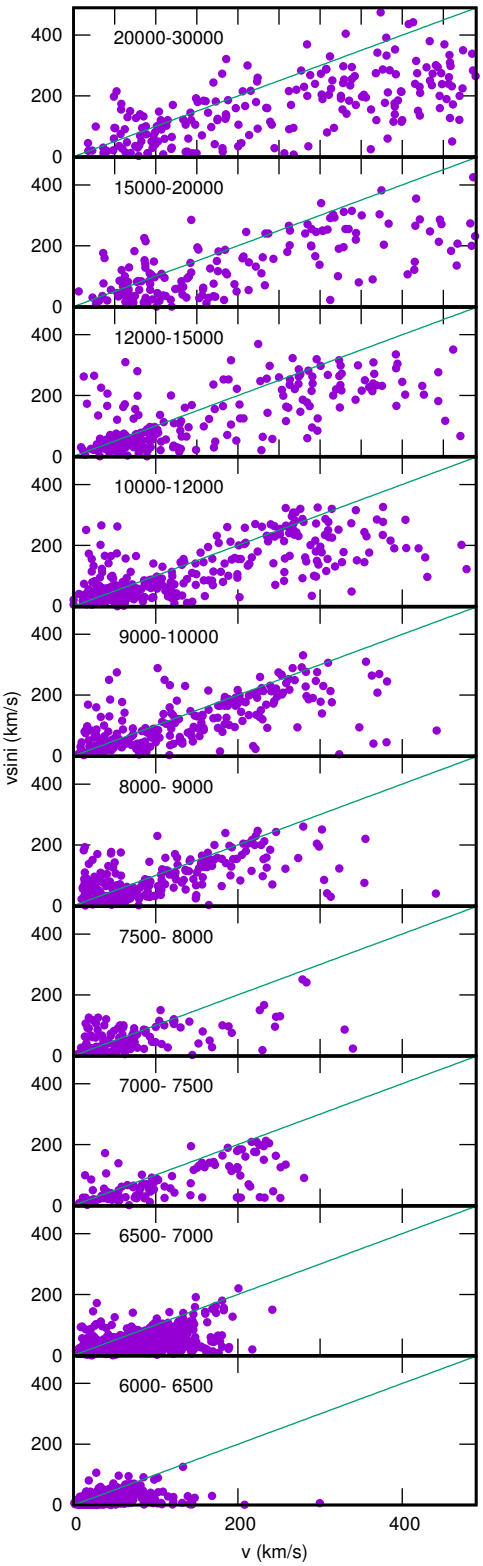

Figure 1. The projected rotation velocity, $v \sin i$, as a function of the equatorial rotation velocity, v, estimated from the photometric period for stars with effective temperature ranges shown in the panels. All main sequence stars ($\log L/L_\odot - (\log L/L_\odot)_{\rm ZAMS} < 1$) with (including Am, Ap, Bp and Be stars) are shown.

$30\,{\rm km\,s^{-1}}$, but varies widely depending on the dispersion used.

The results presented here are from 34,376 stars with photometric periods typical of their rotation periods and classified as ROT, ACV or SXARI variables. This consists of 29,962 *TESS* stars, 3,195 stars from *Kepler* and 1,219 *K2* stars. By contrast, there are only 5,240 stars hotter than 6000 K with reliable $v \sin i$ measurements. Results from rotational light modulation are not only more numerous, but do not require statistical deconvolution to obtain the distribution of equatorial rotational velocities.

3 ROTATION ALONG THE MAIN SEQUENCE

The simplest way of demonstrating that the photometric period is the same as the rotation period is to plot $v \sin i$ as a function of v. Such a plot should show a scatter of points below the $\sin i = 1$ line. If one assumes random orientation of the axes of rotation, more stars will be observed equator-on than pole-on because the distribution in i is equal to $\sin i$. Most points in a plot of $v \sin i$ as a function of v should cluster just below the $\sin i = 1$ line.

In Fig. 1 we show stars for which both v and $v \sin i$ are known. It is clear that the equatorial rotational velocity determined from photometry is generally below $v \sin i$, as expected. Due to errors in v and $v \sin i$, it is quite reasonable to expect some points to lie above the $\sin i = 1$ line, especially at low values of v where higher precision is required for $v \sin i$ measurements and where contamination by possible eclipsing systems is expected to be largest.

If the inclination angles are randomly orientated, one could test that they obeys a $\sin i$ distribution. Unfortunately, the distribution of i from rotational light modulation cannot be random because no light modulation can occur if the star is pole-on. Therefore such a test would not be valid. In any case, the error in i would be around 15° which is too large to be useful for any single star.

There is another test that can be made to determine whether the photometric periods correspond to the rotational periods. One can compare the distribution of v in a limited effective temperature range with the distribution of $v \sin i$ in the same $T_{\rm eff}$ range. This test is independent of the correlation between v and $v \sin i$. Note that, unlike the previous test, the stars chosen to calculate the $v \sin i$ distribution need not be the same as the stars for which v is known.

These distributions are shown in Figs. 2 where Be stars are excluded. It is clear that the distribution of v closely resembles that of $v \sin i$. This is to be expected as most stars would be observed at high angles of inclination. When Be stars are included (Fig. 3), the distributions of v and $v \sin i$ do not agree very well for the hottest stars.

The reason why it is necessary to exclude Be stars from the distribution has to do with their rapid rotation and the fact that the rotational amplitude is much higher than in non-Be stars. It is suspected that rotational modulation in Be stars is a result of obscuration by trapped co-rotating clouds (Balona 2003; Balona & Ozuyar 2020, 2021). This mechanism has different statistical properties from rotational modulation due to starspots.

Table 1 lists the numbers of stars and the mean values $\langle v \rangle$ and $\langle v \sin i \rangle$ for each effective temperature range. The

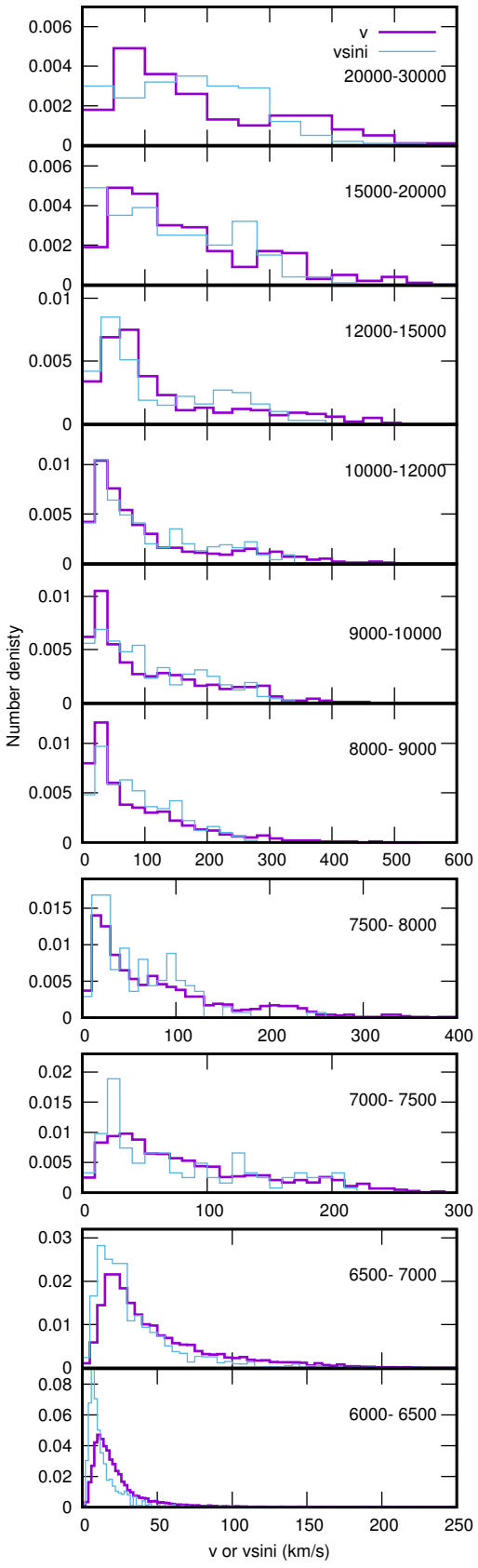

Figure 2. The distribution of equatorial rotational velocities, v (heavy magenta histogram), as determined from photometric periods and the distribution of projected rotation velocities, $v \sin i$ (light blue histogram), for main sequence stars in different $T_{\rm eff}$ ranges. All stars with $T_{\rm eff} < 10000$ K (including Am, Ap, Bp are included, but Be stars are excluded.

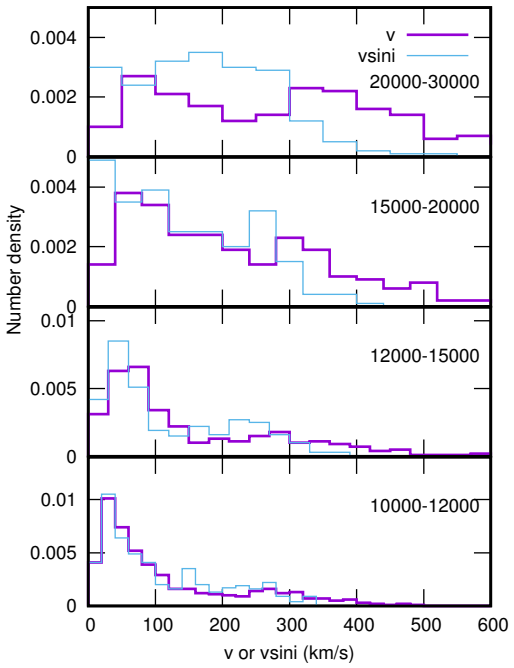

Figure 3. The same as Fig. 2, but for stars with $T_{\rm eff} > 10000$ K. All stars (including Bp and Be stars) are included.

Table 1. The number of stars with known photometric periods, N, in the given effective temperature range, $T_{\rm eff}$. The mean rotational equatorial velocity $\langle v \rangle$ is also listed. The number of stars with $v \sin i$ measurements is given by n. The mean projected rotational velocity is $\langle v \sin i \rangle$. In the bottom section, Be stars are omitted.

$T_{\rm eff}$	N	$\langle v \rangle$	n	$\langle v \sin i \rangle$
Be stars excluded:				
6000-6500	13834	24.1 ± 0.2	2157	12.8 ± 0.2
6500-7000	10387	49.4 ± 0.4	1138	33.5 ± 0.8
7000-7500	2548	85.2 ± 1.3	116	76.9 ± 5.5
7500-8000	1347	83.8 ± 2.1	132	58.7 ± 3.9
8000-9000	2259	88.1 ± 1.8	245	86.8 ± 4.0
9000-10000	1370	110.3 ± 2.6	252	107.5 ± 5.1
10000-12000	1121	112.9 ± 3.2	314	102.8 ± 4.9
12000-15000	538	128.3 ± 4.8	202	105.8 ± 6.4
15000-20000	247	169.8 ± 7.9	130	103.6 ± 6.8
20000-30000	298	190.2 ± 8.2	130	119.5 ± 7.8
Be stars included:				
10000-12000	1155	119.1 ± 3.3	331	106.9 ± 4.8
12000-15000	608	150.2 ± 5.2	235	121.9 ± 6.3
15000-20000	329	215.9 ± 8.2	177	137.7 ± 7.3
20000-30000	539	296.0 ± 8.3	255	174.7 ± 6.6

number of stars in the two highest temperature ranges is still quite small because early B stars are very rare.

Table 2 lists the numbers of ROT stars and the number of main sequence stars (excluding Be stars) for each effective temperature range. In order to obtain some degree of completeness, only stars brighter than 10-th magnitude were used. Fig. 4 shows the fraction of ROT stars as a function of $T_{\rm eff}$. It is not clear whether the variation is real, but one can

Table 2. The number of rotationally variable stars brighter than 10-th magnitude, n, and the number of main sequence stars (excluding Be stars) brighter than 10-th magnitude, N, as a function of effective temperature, $T_{\rm eff}$. The fraction of rotationally variable stars is given by n/N. The number of Be stars, n_e, and the fraction of Be stars $n_e/(N+n_e)$ is shown in the last two columns.

$T_{\rm eff}$	n	N	$\frac{n}{N}$	n_e	$\frac{n_e}{N+n_e}$
6000-6500	6085	19736	0.308		
6500-7000	5898	14842	0.397		
7000-7500	1378	5997	0.230		
7500-8000	733	4135	0.177		
8000-9000	1271	5507	0.231		
9000-10000	866	2443	0.363		
10000-12000	877	1802	0.487	53	0.029
12000-15000	463	858	0.540	119	0.122
15000-20000	201	565	0.356	132	0.189
20000-30000	189	721	0.262	381	0.346

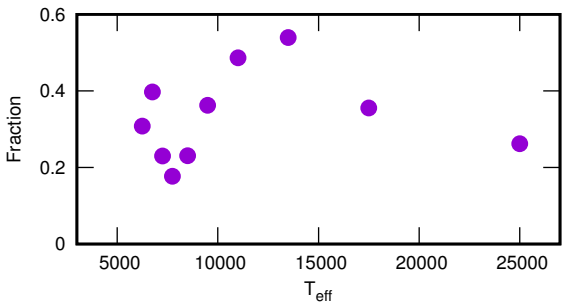

Figure 4. The fraction of rotational variables (excluding Be stars) as a function of effective temperature.

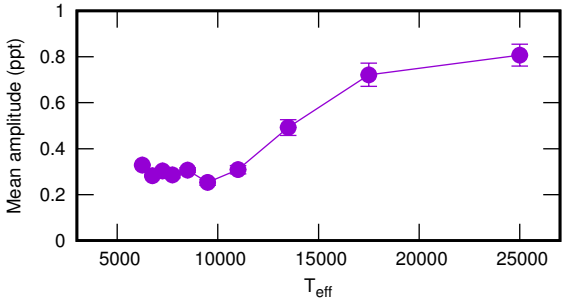

Figure 5. The mean amplitude of rotational variables (excluding ACV, SXARI and Be stars) as a function of effective temperature. 1-σ error bars are shown.

certainly conclude that rotational variability is very common at around 30–40 percent of all main sequence stars. This is a lower limit set by the sensitivity of the detectors and particularly by the detection limit of *TESS* which contributes the most stars to the statistics. It is interesting that the greatest number of ROT stars occurs around early A and late B, where hydrogen is partially ionized at the surface. Whether this is relevant remains to be seen.

3.1 Amplitudes

The mean amplitude of ROT variables (excluding ACV, SXARI and Be stars) as a function of effective temperature is shown in Fig. 5. In this figure only *TESS* data are used to ensure uniformity of detection level. Obviously, the detection level itself will depend on the brightness of the star, but one can assume that the figure might be a reasonable approximation because the distribution in $T_{\rm eff}$ should not depend on brightness.

The rapid increase in amplitude from late- to early-B stars has been previously noted by Balona & Ozuyar (2021), but no explanation was proposed. A possible reason for this increase will be discussed later. Note that the typical rotational amplitude is low, about 0.5 ppt, much lower than the maximum amplitude of 10 ppt used for the definition of ROT variables.

The amplitude distributions of ROT stars (excluding ACV, SXARI and Be stars) are shown in Fig. 6. The difference in amplitude distributions between the A and the early B stars is quite remarkable. The amplitude tail of F and A stars does not extend beyond 0.5 ppt, but from late to early stars the tail becomes progressively extended, reaching to 1 ppt for the hottest stars. There is clearly something happening in the B stars which tends to increase the rotational modulation amplitudes with increasing temperature. This will be discussed later.

4 PECULIAR STARS

4.1 Am and Ap/Bp stars

The Am (metallic-line A stars) are main-sequence A stars with enhanced metal lines in their spectra. The spectral type estimated from the metal lines alone is later than that estimated from the strength of the hydrogen lines. Am stars show significant underabundances of Ca and Sc, and enhanced abundances of Ti and Fe-group elements. The abnormal metal abundance at the surface is thought to be a result of diffusion (Michaud et al. 1983; Turcotte et al. 2000). The late B-type HgMn stars may be considered as the hot analogue of Am stars.

Diffusion is also active in the Ap stars, which have overabundances of Sr, Cr and Eu. The hotter Bp stars are overabundant in Si or Si and Sr. In Am/HgMn stars, where the surface magnetic field is weak or absent, the abundance anomalies are uniformly distributed on the surface. The presence of a strong global magnetic field in Ap/Bp stars leads to non-uniform abundance patches.

Rotational light modulation due to chemical spots is often detected in Ap stars. These are known as α CVn (ACV) variables in the GCVS. In the Bp stars, these are known as SX Ari (SXARI) variables. We have taken $T_{\rm eff} \approx 10,000$ K as the boundary between ACV and SXARI variables.

In the absence of surface mixing such as convection, all stars should have abnormal abundances. In A and B stars with radiative envelopes, another source of mixing needs to be active. This is presumed to be mixing caused by meridional circulation due to rotation. Therefore the Am/HgMn and Ap/Bp stars should be slow rotators, while normal stars should have higher rotation rates. In fact, no normal star should be slowly rotating and there ought to be a distinct

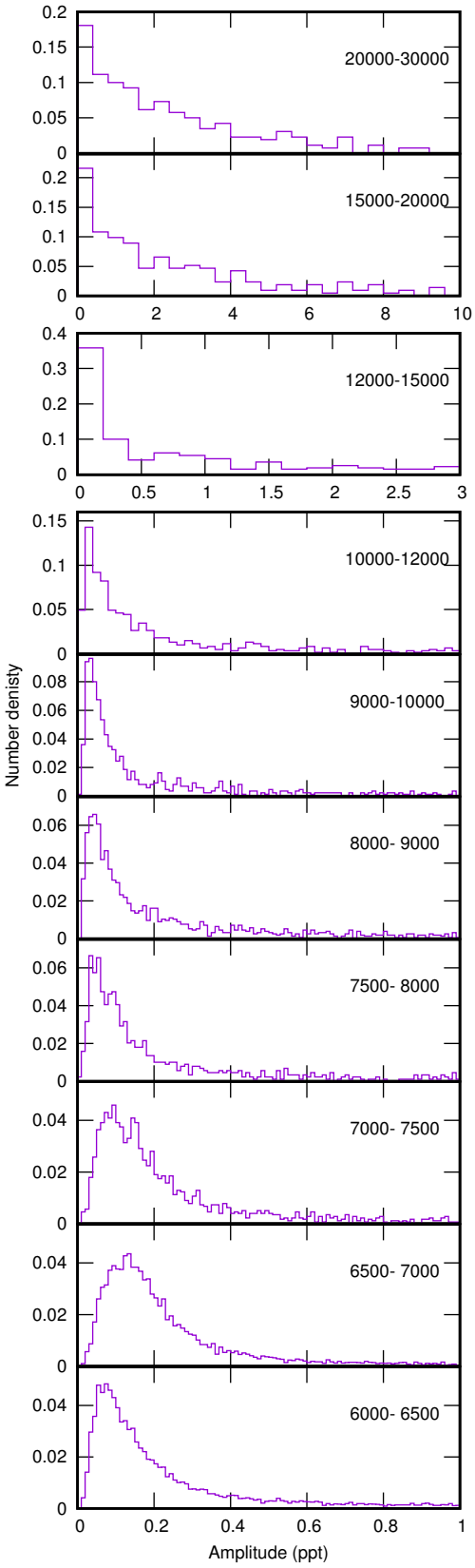

Figure 6. The amplitude distribution of rotational peaks (excluding Ap, Bp and Be stars) in different effective temperature ranges (as labeled).

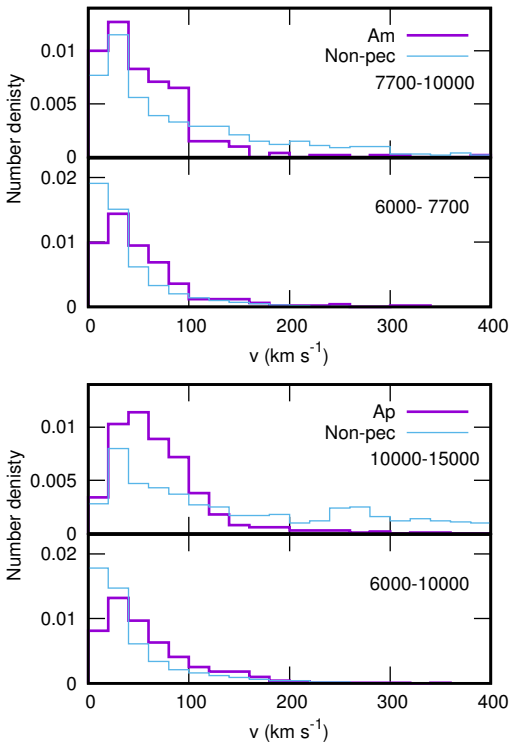

Figure 7. The distribution of equatorial rotational velocities, v, of Am stars (top two panels) and Ap stars (bottom two panels) in two effective temperature ranges. The heavy magenta histograms are for Am or Ap/Bp stars, while the light blue histograms are for non-peculiar stars.

separation in the rotation rates of peculiar and normal stars. Indeed, early studies indicated the expected bimodal $v \sin i$ distribution in A stars (Conti 1965; Abt & Morrell 1995). Some caution is required in accepting this conclusion owing to the small samples involved.

More recently, Royer et al. (2007) found a bimodal distribution of rotation velocities among A stars which is attributed to angular momentum loss during stellar evolution (i.e. unrelated to chemical peculiarity). Zorec & Royer (2012) find a uni-modal equatorial rotational velocity distribution for stars less massive than 2.5 $M_\odot$. Qin et al. (2021) analysed a sample of 21 Am stars and 178 normal A stars, all having photometric rotational modulation, but could find no difference in either the rotational period or the average rotational light amplitude between Am and normal A stars.

In Fig. 7 the distribution of equatorial rotational velocities, v, for Am and Ap/Bp stars in two different effective temperature ranges is compared to that for non-peculiar stars. There appears to be no difference in rotational properties between non-peculiar and peculiar stars (both Am and Ap) in the cooler temperature ranges. For higher $T_{\rm eff}$, the peculiar stars do seem to rotate, on average, somewhat more slowly than non-peculiar stars. This is confirmed by the mean values of $\langle v \rangle$ and $\langle v \sin i \rangle$ shown in Table 3.

Out of 130 HgMn stars in our catalogue, 55 were detected as rotational variables. This number is too small to determine the v or $v \sin i$ distributions, but the mean values in Table 3 suggest that HgMn stars, on average, do rotate

Table 3. The number of stars, N, the mean equatorial rotational velocities, $\langle v \rangle$ and the mean projected rotational velocities, $\langle v \sin i \rangle$, for Am, HgMn, and Ap/Bp stars compared to non-peculiar stars in the given effective temperature ranges. The statistics for classical Be stars are shown in the last few rows.

Description	Quantity	N	km s^{-1}
6000–7700 K:			
Am	$\langle v \rangle$	247	55.1 ± 3.1
Non-pec	$\langle v \rangle$	18735	40.5 ± 0.3
Am	$\langle v \sin i \rangle$	54	44.6 ± 4.5
Non-pec	$\langle v \sin i \rangle$	2683	22.7 ± 0.5
7700–10000 K:			
Am	$\langle v \rangle$	260	56.9 ± 3.0
Non-pec	$\langle v \rangle$	2422	96.6 ± 1.9
Am	$\langle v \sin i \rangle$	80	53.4 ± 4.7
Non-pec	$\langle v \sin i \rangle$	276	104.1 ± 4.3
10000-15000 K:			
HgMn	$\langle v \rangle$	55	72.8 ± 9.3
Non-pec	$\langle v \rangle$	1671	117.4 ± 2.6
HgMn	$\langle v \sin i \rangle$	52	47.0 ± 6.1
Non-pec	$\langle v \sin i \rangle$	526	103.0 ± 3.8
Ap:			
6000–10000 K:			
Ap	$\langle v \rangle$	670	61.4 ± 1.9
Non-pec	$\langle v \rangle$	21157	46.9 ± 0.4
Ap	$\langle v \sin i \rangle$	165	36.9 ± 2.7
Non-pec	$\langle v \sin i \rangle$	2959	30.3 ± 0.7
10000–15000 K:			
Ap	$\langle v \rangle$	598	70.8 ± 2.1
Non-pec	$\langle v \rangle$	774	152.4 ± 4.4
Ap	$\langle v \sin i \rangle$	183	47.5 ± 2.9
Non-pec	$\langle v \sin i \rangle$	244	145.1 ± 6.0
10000-20000 K:			
Be	$\langle v \rangle$	233	325.2 ± 9.0
Be	$\langle v \sin i \rangle$	107	217.3 ± 7.6
Be	$\langle v/v_{\rm crit} \rangle$	233	0.71 ± 0.02
20000-30000 K:			
Be	$\langle v \rangle$	282	410.9 ± 10.1
Be	$\langle v \sin i \rangle$	133	226.9 ± 8.0
Be	$\langle v/v_{\rm crit} \rangle$	238	0.73 ± 0.02

more slowly than non-peculiar stars in the same temperature range.

What is important is that there is no clear separation in the rotation rates of normal and chemically peculiar stars. Although mean values might differ, most normal stars are slow or moderate rotators (i.e., $v < 100\,\mathrm{km\,s^{-1}}$), as shown in Fig. 7, and the same is true for chemically peculiar stars. There is no evidence to indicate that rotation plays any important role in suppressing the diffusion process.

There are 560 Am δ Sct or γ Dor stars among 3614 Am stars brighter than 10-th magnitude. Therefore about 15 percent of Am stars pulsate. This is not too different from the 19 percent of normal stars or the 17 percent of Ap stars which pulsate (Balona 2022). Clearly, pulsation does not play an important role in this process either.

4.2 Be stars

Be stars vary on many time scales. Practically all Be stars show large irregular light variations due to circumstellar material. In addition, short-period (0.5–2.0 d) light and line profile variations are present in some, but not all, Be stars (Walker 1953; Baade 1979, 1982). These have been usually interpreted as non-radial pulsation (NRP). *TESS* observations indicate that about 75 percent of Be stars have short-period variations. However, these are not strictly periodic (Balona & Ozuyar 2020, 2021).

A distinct pattern in the periodograms of Be stars has been found (see Fig. 1 in Balona & Ozuyar 2021). This consists of a peak near zero frequency which is attributed to circumstellar material. Two other systems of broad peaks are generally visible: the rotational peak and its harmonic. From this pattern, the presumed rotation period can be measured. It should be noted that the rotational peak is often broad and sometimes multiple, so that the estimated rotational frequency is uncertain by perhaps $0.1\,\mathrm{d^{-1}}$.

The resulting relationship between v and $v \sin i$ in Be stars shows that the photometric period is close or equal to the rotation period. These results, as well as other well-known properties of Be stars, can be explained by the the impulsive magnetic rotator model (Balona 2003; Balona & Ozuyar 2020, 2021). In this model activity at the surface ejects material which is trapped at diametrically opposite locations where the geometric and magnetic equators intersect. The proposed magnetic field can be very weak, perhaps only a few gauss. The trapped material is eventually dispersed into the circumstellar disk.

The distinctive light curves and periodograms of Be stars are quite different from those of the pulsating SPB or γ Dor stars, which have about the same periods as Be stars. Obscuration due to trapped gas clouds can be large and lead to high-amplitude, almost eclipse-like, light variations (see Balona & Ozuyar 2021). This is why the short-period light and line profile variations in Be stars are easily seen from the ground. Because of rapid changes in the amount of trapped gas, the light variations are not expected to be strictly periodic, unlike pulsations.

Because of the effect of circumstellar material, it is difficult to obtain reliable effective temperature estimates for Be stars. The use of spectral classification to estimate $T_{\rm eff}$ is probably the safest option as it avoids systematic effects. The less precise temperature estimate increases the error in v to about $50\,\mathrm{km\,s^{-1}}$.

The top panels of Fig. 8 show that the rotation period estimates for Be stars are consistent with their rotation periods. The middle panels show the distribution of v and $v \sin i$, while the bottom panels show the distribution of $v/v_{\rm crit}$, where $v_{\rm crit}$ is the critical rotational velocity. The critical rotational velocity for each star was estimated using the mass derived from $T_{\rm eff}$ and the stellar radius and the calibration in Torres et al. (2010). Table 3 lists the statistics. The error of $v/v_{\rm crit}$ for individual stars is, naturally, rather large (probably around 0.1), which is why values sometimes exceed $v/v_{\rm crit} > 1$.

It is evident that Be stars rotate at much less than $v/v_{\rm crit} > 0.95$, the value necessary for NRP to produce sufficient momentum transfer for mass ejection (Townsend et al. 2004). The approximate value derived here is about $v/v_{\rm crit} =$

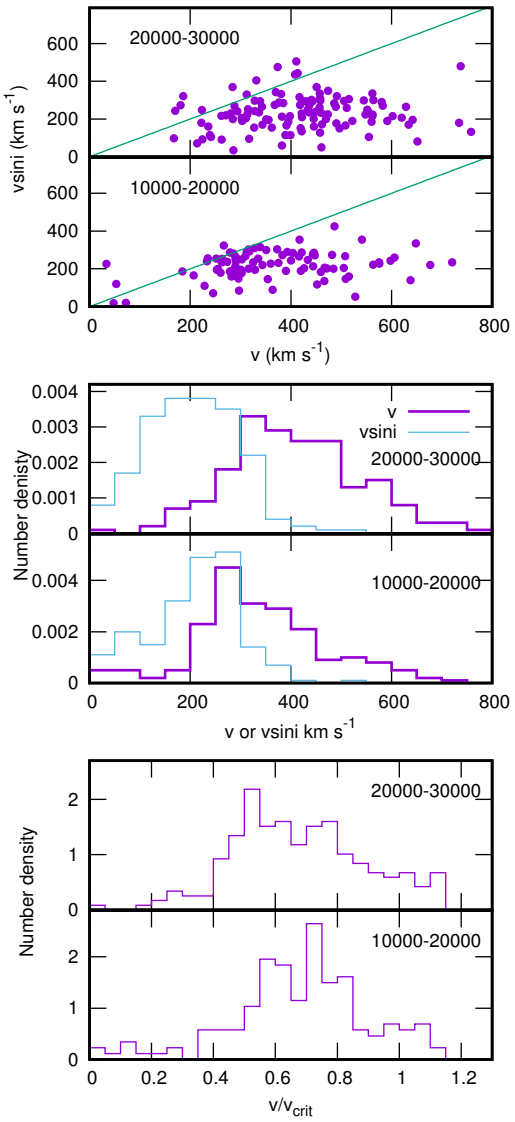

Figure 8. The top panels show the projected rotational velocity, $v \sin i$, as a function of the equatorial rotational velocity, v, for Be stars in two different effective temperature ranges. The middle panel shows the distributions of v and $v \sin i$. The bottom panels shows the distribution of the ratio $v/v_{\rm crit}$, where $v_{\rm crit}$ is the critical rotation velocity.

0.72, which is in line with estimates based on deconvolution of $v \sin i$ (Frémat et al. 2005; Cranmer 2005; Zorec et al. 2016).

5 DISCUSSION AND CONCLUSIONS

From space photometry it is shown that at least 30 percent of main sequence A and B stars vary in light with periods indistinguishable from their rotational periods. This fraction is a lower limit because the rotational light amplitude of many stars may be too small to be detectable. The rotational variables or ROT stars are by far the most common type of variable among the A and B stars.

Let us suppose that what we are observing is not rotational modulation but pulsation. The periods are observed to be close or equal to the rotation period over a very wide range of effective temperatures. This rules out pulsation driven by an opacity mechanism, because this operates only in limited effective temperature ranges. Inertial r modes, as discussed by Saio et al. (2018), may explain the "hump" in the "hump and spike" feature seen in the periodograms of many A stars (Balona 2014; Trust et al. 2020). These are only visible in long time series such as *Kepler* and are given the ROTD classification in Balona et al. (2015) and later publications. While Saio et al. (2018) attribute the broad "hump" to r modes, rotational modulation is still needed to explain the sharp "spike". The fact that rotational light modulation in addition to r modes is required to explain ROTD variables, clearly invalidates pulsation as the sole cause for light modulation in these stars.

Grazing eclipses, eclipses by compact objects or planets seem an attractive alternative to explain these results. However, there is no reason why the orbital periods of these systems should correspond so closely with the rotation periods. The large fraction of ROT stars is also at variance with this idea. The larger the area covered by the eclipse, the larger the amplitude of the eclipse. Since the probability of an eclipse increases with the area that is occulted, the number of grazing eclipses should increase with increasing amplitude. However, as Fig. 6 shows, the opposite is observed. We may rule out eclipses as the cause of ROT variables.

Magnetically trapped, co-rotating clouds is the explanation for the short-period light variations in Be stars proposed by Balona (2003); Balona & Ozuyar (2020) and Balona & Ozuyar (2021). In this impulsive magnetic rotator model, energy released from magnetic reconnection (flares) is responsible for ejection of material. This material eventually migrates to one or two diametrically opposed regions where the geometric and magnetic equators intersect. It is these magnetically trapped clouds which are presumed to produce the observed light and line profile variations. The model explains the the characteristic periodogram and light curve as well as several other features of Be stars.

From the distribution of Be star equatorial rotational velocities, the ratio of equatorial to critical rotation, $v/v_{\rm crit}$, is derived. Be stars show a wide variation in this ratio with mean $v/v_{\rm crit} = 0.71$. This value agrees with several studies involving studies of the $v \sin i$ distribution (Frémat et al. 2005; Cranmer 2005; Zorec et al. 2016). However, it is well below the value $v/v_{\rm crit} > 0.95$ required for mass ejection from nonradial pulsation (Townsend et al. 2004). In any case, the incoherent nature of the periodicity is inconsistent with pulsation.

It is found that the rotational modulation amplitude and amplitude range in non-Be stars increases rapidly from late-B to early-B stars (Figs. 5 and 6). The increase in amplitude mimics the increase in relative numbers of Be stars with increasing effective temperature. It is suggested that both these effects could be due to an increase of incipient Be stars (i.e. Be stars with very weak or undetectable emission) in the sample of non-Be stars. The light modulation amplitude due to trapped clouds is much larger than the amplitude from starspots. The greater the proportion of incipient B stars in the sample, the larger the light amplitude. This would also tend to increase the range of observed amplitudes with effective temperature, as observed.

The Sun's global magnetic field is only about 2 G, which

would be difficult to detect at stellar distances. There are, indeed, 56 Be stars where magnetic fields have been detected, with effective field strengths in the range 11–1821 G. However, the error in these measurements is typically 30–1500 G. Therefore there is no reason to presume that global magnetic fields with strengths similar to that in the Sun are not present in Be stars. This would be sufficient to trap ejected ionized material.

It is well known that irregular activity outbursts are a feature of Be stars and that Be stars can lose their emission from time to time. This supports irregular activity cycles of mass ejection, possibly driven by magnetic reconnection (flaring), as in the Sun. If starspots are present in A and B stars, then it follows that flares may be expected to occur. Indeed, there is evidence that flares in A stars have been observed (Balona 2013, 2015, 2021; Qin et al. 2021). The idea that the flares are to be associated with a late-type companion and not the A star itself (Pedersen et al. 2017) is reasonable, but does not address the considerably higher energies associated with the observed flares.

Cantiello et al. (2009); Cantiello & Braithwaite (2011); Cantiello et al. (2011); Cantiello & Braithwaite (2019) have explored sub-surface convective zones in A and B stars. They conclude that the majority of intermediate-mass stars should have dynamo-generated magnetic fields with a strength of a few Gauss at the surface. These magnetic fields can appear at the surface as bright spots and cause photometric variability via rotational modulation. It is not clear whether the observations support this idea. The presence sub-surface convection depends on the effective temperature and one would have expected regions where no sub-surface convection is present, but rotational modulation seems to occur, unbroken, all along the main sequence. One would also have expected a region of little or no rotational modulation where dark spots transition into bright spots, but there is no evidence for this in the observations. More detailed predictions are required to fully test this proposal.

In this paper we also investigate the effect of rotation on chemically peculiar stars. The diffusion hypothesis has been highly successful in describing the surface abundance anomalies in Am, Ap and Bp stars. There is no doubt that gravitational settling and radiative acceleration must occur in the atmospheres of all stars, but surface convection causes mixing and destroys the diffusion process, leading to normal surface abundances. The question that has to be answered is what causes mixing in stars with radiative atmospheres? The answer is thought to be mixing of the upper layers through meridional circulation induced by rotation. The prediction is that all peculiar stars should be slow rotators, while non-peculiar stars should rotate more rapidly.

As Fig. 7 shows, most of the non-peculiar stars rotate just as slowly as the peculiar Am, Ap and Bp stars. There is no distinct separation in the rotation rate of peculiar and non-peculiar stars in any temperature range. This shows that rotation has little, if any, effect in suppressing diffusion. There must be other factors which mix the upper layers and prevent the abundance anomalies. If surface convection is more prevalent in A and B stars than previously supposed, it offers a possible mechanism for mixing of surface layers and suppressing diffusion in non-peculiar stars.

The overall conclusion is that the atmospheres of A and B stars are considerably more active than previously supposed. It is almost as though quiescent radiative atmospheres are merely a theoretical construct which do not exist in reality. The results presented here points to the presence of thermal starspots, similar to those in the Sun, in all main sequence stars from late M to early B-type stars. Further progress would require detailed high-resolution spectroscopy of a few hot A or B stars showing rotational light modulation. These observations could determine if the spots are dark or bright and possibly information of their sizes and structure.

ACKNOWLEDGMENTS

LAB wishes to thank the National Research Foundation of South Africa for financial support.

This paper includes data collected by the *TESS* mission. Funding for the *TESS* mission is provided by the NASA Explorer Program. Funding for the *TESS* Asteroseismic Science Operations Centre is provided by the Danish National Research Foundation (Grant agreement no.: DNRF106), ESA PRODEX (PEA 4000119301) and Stellar Astrophysics Centre (SAC) at Aarhus University. We thank the *TESS* and TASC/TASOC teams for their support of the present work.

This work has made use of data from the European Space Agency (ESA) mission *Gaia* (https://www.cosmos.esa.int/gaia), processed by the *Gaia* Data Processing and Analysis Consortium (DPAC, https://www.cosmos.esa.int/web/gaia/dpac/consortium). Funding for the DPAC has been provided by national institutions, in particular the institutions participating in the *Gaia* Multilateral Agreement. This research has made use of the SIMBAD database, operated at CDS, Strasbourg, France.

The data presented in this paper were obtained from the Mikulski Archive for Space Telescopes (MAST). STScI is operated by the Association of Universities for Research in Astronomy, Inc., under NASA contract NAS5-2655.

DATA AVAILABILITY

A catalogue of stars with variability classification of *Kepler, K2* and em TESS stars by the author is in preparation. In the meantime, data underlying this article will be shared on reasonable request to the corresponding author.

REFERENCES

Abt H. A., Morrell N. I., 1995, ApJS, 99, 135
Anders F., Khalatyan A., Queiroz A. B. A., et al., 2022, A&A, 658, A91
Baade D., 1979, The Messenger, 19, 4
—, 1982, A&A, 105, 65
Balona L. A., 2003, in Astronomical Society of the Pacific Conference Series, Vol. 305, Astronomical Society of the Pacific Conference Series, L. A. Balona, H. F. Henrichs, & R. Medupe, ed., p. 263
—, 2011, MNRAS, 415, 1691
—, 2013, MNRAS, 431, 2240
—, 2014, MNRAS, 441, 3543
—, 2015, MNRAS, 447, 2714
—, 2016, MNRAS, 457, 3724

—, 2017, MNRAS, 467, 1830
—, 2019, MNRAS, 490, 2112
—, 2021, Frontiers in Astronomy and Space Sciences, 8, 32
—, 2022, MNRAS, 510, 5743
Balona L. A., Abedigamba O. P., 2016, MNRAS, 461, 497
Balona L. A., Baran A. S., Daszyńska-Daszkiewicz J., De Cat P., 2015, MNRAS, 451, 1445
Balona L. A., Handler G., Chowdhury S., et al., 2019, MNRAS, 485, 3457
Balona L. A., Ozuyar D., 2020, MNRAS, 493, 2528
—, 2021, ApJ, 921, 5
Baran A. S., Koen C., 2021, Acta Astron., 71, 113
Baran A. S., Koen C., Pokrzywka B., 2015, MNRAS, 448, L16
Bowman D. M., Michielsen M., 2021, A&A, 656, A158
Braithwaite J., Spruit H. C., 2004, Nature, 431, 819
Breger M., Stich J., Garrido R., et al., 1993, A&A, 271, 482
Brown T. M., Latham D. W., Everett M. E., Esquerdo G. A., 2011, AJ, 142, 112
Cantiello M., Braithwaite J., 2011, A&A, 534, A140
—, 2019, ApJ, 883, 106
Cantiello M., Braithwaite J., Brandenburg A., Del Sordo F., Käpylä P., Langer N., 2011, in IAU Symposium, Vol. 272, Active OB Stars: Structure, Evolution, Mass Loss, and Critical Limits, Neiner C., Wade G., Meynet G., Peters G., eds., pp. 32–37
Cantiello M., Langer N., Brott I., et al., 2009, A&A, 499, 279
Charbonneau P., 2014, ARA&A, 52, 251
Chen Y., Girardi L., Fu X., et al., 2019, A&A, 632, A105
Conti P. S., 1965, ApJ, 142, 1594
Cranmer S. R., 2005, ApJ, 634, 585
Frémat Y., Zorec J., Hubert A.-M., Floquet M., 2005, A&A, 440, 305
Gaia Collaboration, Prusti T., de Bruijne J. H. J., et al., 2016, A&A, 595, A1
Gaia Collaboration, Vallenari A., Brown A. G. A., et al., 2022, arXiv e-prints, arXiv:2208.00211
Głębocki R., Gnaciński P., 2005, in ESA Special Publication, Vol. 560, 13th Cambridge Workshop on Cool Stars, Stellar Systems and the Sun, Favata F., Hussain G. A. J., Battrick B., eds., p. 571
Gontcharov G. A., 2017, Astronomy Letters, 43, 472
Green G. M., Schlafly E., Zucker C., Speagle J. S., Finkbeiner D., 2019, ApJ, 887, 93
Hall D. S., 1972, PASP, 84, 323
Michaud G., 1980, AJ, 85, 589
Michaud G., Charland Y., Vauclair S., Vauclair G., 1976, ApJ, 210, 447
Michaud G., Tarasick D., Charland Y., Pelletier C., 1983, ApJ, 269, 239
Pedersen M. G., Antoci V., Korhonen H., White T. R., Jessen-Hansen J., Lehtinen J., Nikbakhsh S., Viuho J., 2017, MNRAS, 466, 3060
Qin L., Luo A. L., Hou W., et al., 2021, AJ, 162, 32
Royer F., Zorec J., Gómez A. E., 2007, A&A, 463, 671
Saio H., Kurtz D. W., Murphy S. J., Antoci V. L., Lee U., 2018, MNRAS, 474, 2774
Samus N. N., Kazarovets E. V., Kireeva N. N., Pastukhova E. N., Durlevich O. V., 2018, in Stars and Satellites, Proceedings of the Memorial Conference Devoted to A.G. Masevich 100th Anniversary, Shustov B. M., Wiebe D. S., eds., pp. 358–361
Sikora J., Wade G. A., Rowe J., 2020, MNRAS, 498, 2456
Stassun K. G., Oelkers R. J., Pepper J., et al., 2018, AJ, 156, 102
Strassmeier K. G., 2009, 2009AARv..17..251S, 390, 1701
Torres G., Andersen J., Giménez A., 2010, A&ARv, 18, 67
Townsend R. H. D., Owocki S. P., Howarth I. D., 2004, MNRAS, 350, 189
Trust O., Jurua E., De Cat P., Joshi S., 2020, MNRAS, 492, 3143
Turcotte S., Richer J., Michaud G., Christensen-Dalsgaard J., 2000, A&A, 360, 603
Vanderburg A., Johnson J. A., 2014, PASP, 126, 948
Walker M. F., 1953, ApJ, 118, 481
Zorec J., Frémat Y., Domiciano de Souza A., et al., 2016, A&A, 595, A132
Zorec J., Royer F., 2012, A&A, 537, A120